Centralized and distributed Model Predictive Control for the maximization of the thermal power of solar parabolic-trough plants

José Ramón D. Frejo and Eduardo F. Camacho

Dept. de Ingeniería de Sistemas y Automática, University of Seville, Spain, e-mails: jdominguez3@us.es, efcamacho@us.es

Abstract

This paper proposes a new centralized Model Predictive Control (MPC) algorithm for the maximization of the thermal power obtained with a parabolic-trough collector field. The optimal operation of the plant is achieved by controlling a set of valves located at the beginning of each loop of collectors, which allow to outperform the response achieved with traditional control approaches for parabolic-trough plants.

Unfortunately, the computational complexity of the proposed MPC controller hinders its application in real-time for medium and large parabolic-trough power plants. Consequently, this paper also proposes a logic-based distributed Model Predictive Control algorithm, which approaches the performance of the centralized MPC but entailing a much lower computational load.

The proposed controllers are tested by simulation using a model of the collector field ACUREX (Almería, Spain) along a 2-hour synthetic DNI profile. The results obtained show that the proposed distributed algorithm is able to perform quite close to the centralized one. Moreover, the analysis of the numerical results (in terms of achieved power) shows that the use of valves at the beginning of each loop substantially improve the achieved thermal power, that the achieved performance using a local controller is significantly lower than using a global one, and that the maximization of the thermal power does not imply the maximization or minimization of the outlet temperature.

Keywords: Solar Energy, Model Predictive Control, Distributed MPC, Parabolic-trough collectors.

1. Introduction

Nowadays, climate change is one of the top challenges for the future of humanity since increase in global average temperature brings disastrous consequences, endangering the survival of the fauna and flora of the Earth, including human beings. The worst climate change impacts include the melting of the ice mass at the poles, rising sea level, producing flooding and threatening coastal environments. [1]

*This research was supported by the European Union's Horizon 2020 research and innovation programee under the ERC Advanced Grant agreement No 789051.

As a consequence, during the last decades, much research has been focused on the use of renewable energies. Since solar energy is the most abundant source of renewable energy, its use has rapidly increased since the 80s. Indeed, many solar electricity production, furnaces, heating and solar cooling systems have been developed in the last decades [2].

The most commonly used technologies for electric production using solar energy are concentrated solar thermal (CST) and photovoltaic (PV) [3]. The main advantage of CST plants with respect to PV plants is the capability of incorporating Thermal Energy Storage (TES), which stores energy in the form of heat (for example, using molten salt), which enables these plants to continue to generate electricity whenever it is needed, whether day or night.

Within CST plants, the most used technologies for concentrating the solar radiation are parabolic-trough collectors, solar towers, Fresnel collector and solar dishes. This paper focuses on the control parabolic-trough collector fields, the CST technology that currently dominates the worldwide market [3].

Many different control structures have been proposed for the operation of parabolic-trough plant [4, 5]: classical PID control, feedforward control, Model Predictive Control (MPC) [6], adaptive control, gain-scheduled control, cascade control, internal model control, time delay compensation, optimal control, non-linear control, robust control, fuzzy logic control and neural network controllers.

However, due to the strong nonlinear behavior of the distributed solar collector field, there are many incentives to use nonlinear MPC strategies (NMPC) [7].

Within the different NMPC approaches proposed for the control of parabolic-though plants, it is worth to mention the controller proposed in [8], which allows to increase solar plant performance and, therefore, reduce investment and operating costs. This improvement is achieved by an on-line determination of optimal operating points in order to maximize electrical production.

However, the performance obtained using the controller proposed in [8] may be improved by taking into account the following considerations:

- In [8], the energy produced is maximized in order to find a set-point for the temperatures, which is used to compute the value of the oil flow rate. However, the integration of both optimizations (i.e. to directly find the values of the oil flow rates that maximize the produced energy) may increase the performance achieved by the controller.

- In [8], and in most of the previous references, it is assumed that, once that the oil flow rate is computed, it is applied to the entire field without the capability of controlling the flow entering each loop. However, if the loops are unbalanced (because of, for example, a different effective radiation affecting to each loop), controlling the oil flow rate that enter each loop can substantially increase the achieved performance.

In [9], the manipulation of the inlet valves of the loops in order to homogenize the loop temperatures is studied. Results show that, if the solar field is not well balanced, a 3.3 - 4.4 % production increment is achieved with respect the case without valves. This strategy uses a common set-point for the outlet temperature of the entire set of loops. As in the case of [8], the achieved performance may be still increased by directly finding the values of the oil flow rates that maximize the produced energy (i.e. without using set-points for the outlet temperature). In [10], a control strategy that manipulates individually the oil flow circulating through each loop is proposed. However, the controller proposed in [10] is not easily applicable to real plants because of the high computational load needed if long horizons are used (around 20 s to simulate a period of 39 s).

Accordingly, the goal of this paper is to propose an MPC strategy that maximizes, by controlling a set of valves located at the beginning of each loop, the thermal power obtained with a parabolic-trough collector field.

Unfortunately, the computational complexity of a centralized MPC that solves this problem makes unfeasible the use of this controller architecture in real-time for large parabolic-trough power plants. In order to deal with this problem, a distributed MPC architecture will be proposed which allows to approach the performance of the centralized MPC with a much lower computational load.

Therefore, the main contributions of this paper are the following:

- The proposal and simulation of a centralized MPC that maximizes the thermal power of a parabolic-trough field taking as decision variables the oil flow rate entering each loop.
- The proposal and simulation of a distributed MPC that approaches the optimal performance and can be computed in real-time.
- To show numerically that, as explained in [9], the use of valves at the beginning of each loop can significantly increase the achieved thermal power and that, as explained in [8], to operate the collector field at the highest outlet temperatures does not implies a larger energy production.

This paper is structured as follows: Firstly, the modeling of a parabolic-though collector field is explained in Section 2. Subsequently, in Section 3, the formulation of a centralized MPC for the maximization of the thermal power of a parabolic-trough plant is presented. In order to reduce the computation load required by the centralized MPC, a distributed MPC approach is proposed in Section 4. Finally, the simulation results for the field of solar collectors ACUREX are presented in Section 5 and the main conclusions are drawn in Section 6.

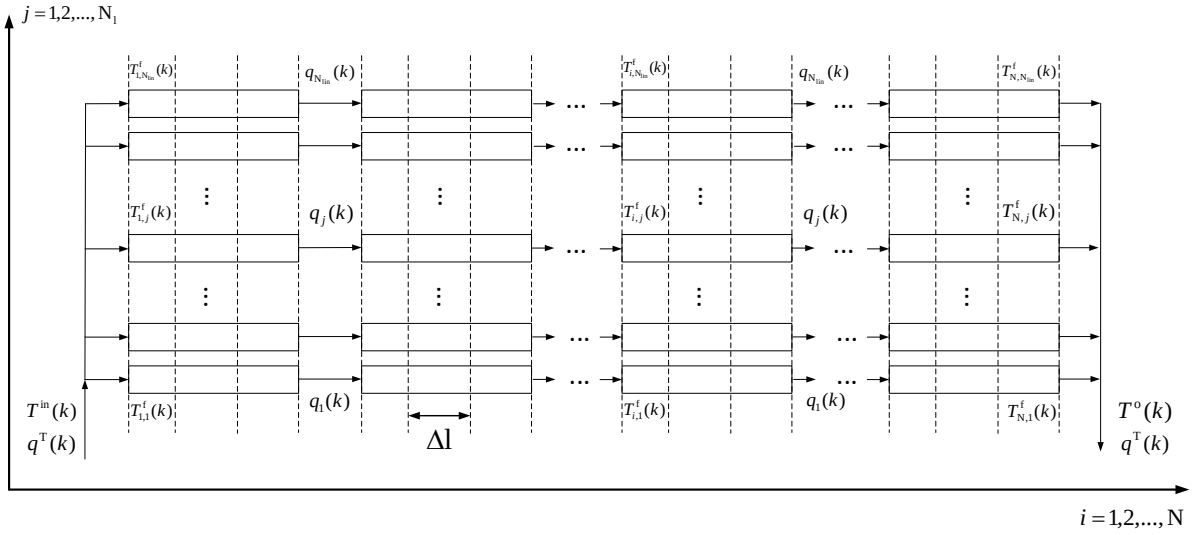

Figure 1: Schematic representation of solar collector field

2. Modeling of Concentrated Solar Plants

2.1. Model structure

A parabolic trough solar plant consists of a collector field, a Power Conversion System (PCS), a Thermal Energy Storage system and auxiliary elements such as pumps, pipes and valves. The solar collector reflects Direct Normal Irradiance (DNI) onto a tube in which a heat transfer fluid, usually synthetic oils, circulates. The oil is heated up and is used by the PCS to produce electricity by means of a turbine. The storage system is necessary to cover the possible mismatch between the solar energy available and the demand.

This paper focuses on the collector field, assuming that the thermal power provided by the collector field is fully transformed into electrical electricity by the PCS and/or stored at the TES.

The whole collector field can be modeled by adding loops in parallel as it can be seen in Figure 1. The collector field is represented as a graph where the N_l links (indexed by j) correspond to collector loops, which are divided into N segments of length Δl.

2.2. Dynamic equations

The Heat Transfer Fluid (HTF) temperature $T^{\mathrm{f}}_{i,j}(k)$, the metal temperature $T^{\mathrm{m}}_{i,j}(k)$ and the auxiliary temperature $T^{\mathrm{lf}}_{i,j}(k-1)$ dynamically characterize the state of each segment i of loop j, where k is the time step corresponding to the time instant $t = k\Delta\mathrm{T}$ and ΔT is the simulation time step.

Three main equations describe the system dynamics of the collector field [4]:

- The first one expresses the energy balance on each segment of the metal:

$$T^{\mathrm{m}}_{i,j}(k) = T^{\mathrm{m}}_{i,j}(k-1) + \frac{\Delta \mathrm{T}}{\rho^{\mathrm{m}} C^{\mathrm{m}} A^{\mathrm{m}}} \Big(\eta^{\mathrm{col}}_{i,j} G_{i,j} I_{i,j}(k) - \pi D^{\mathrm{m}} H^{\mathrm{l}}_{i,j}(k-1) \Big(T^{\mathrm{m}}_{i,j}(k-1) - T^{\mathrm{a}}(k) \Big) - \pi D^{\mathrm{f}} H^{\mathrm{t}}_{i,j}(k-1) \Big(T^{\mathrm{m}}_{i,j}(k-1) - T^{\mathrm{1f}}_{i,j}(k-1) \Big) \Big) \tag{1}$$

where ρ^{m} is the density of the metal, C^{m} is the specific heat capacity of the metal, A^{m} is the cross-sectional area of the pipe, D^{m} is the outer pipe diameter, D^{f} is inner pipe diameter, $\eta^{\mathrm{col}}_{i,j}$ and $G_{i,j}$ are, respectively, the efficiency and the aperture of the collector located on segment i of loop j, $T^{\mathrm{a}}(k)$ is the ambient temperature at time instant $k\Delta\mathrm{T}$, and $I_{i,j}(k)$, $H^{\mathrm{l}}_{i,j}(k-1)$, and $H^{\mathrm{t}}_{i,j}(k-1)$ are, respectively, the corrected DNI, the coefficient of thermal losses, and the convective heat transfer coefficient of pipe interior affecting to segment i of loop j at time instant $(k-1)\Delta\mathrm{T}$.

- The second equation expresses the energy balance on the HTF for each segment of the collector field:

$$T^{\mathrm{f}}_{i,j}(k) = T^{\mathrm{f}}_{i,j}(k-1) + \frac{\pi D^{\mathrm{f}} H^{\mathrm{t}}_{i,j}(k-1)\Delta\mathrm{T}}{\rho^{\mathrm{f}}_{i,j}(k-1) C^{\mathrm{f}}_{i,j}(k-1) A^{\mathrm{f}}} \Big(T^{\mathrm{m}}_{i,j}(k-1) - T^{\mathrm{1f}}_{i,j}(k-1) \Big) \tag{2}$$

where A^{f} is the cross-sectional area of the fluid and $\rho^{\mathrm{f}}_{i,j}(k-1)$ and $C^{\mathrm{f}}_{i,j}(k-1)$ are, respectively, the density and the specific heat capacity of the fluid located on segment i of loop j at time instant $(k-1)\Delta\mathrm{T}$.

- The third equation computes the auxiliary temperature:

$$T^{\mathrm{1f}}_{i,j}(k) = T^{\mathrm{f}}_{i,j}(k) - \frac{q_j(k)\Delta\mathrm{T}}{\Delta\mathrm{l} A^{\mathrm{f}}} \Big(T^{\mathrm{f}}_{i,j}(k) - T^{\mathrm{f}}_{i-1,j}(k) \Big) \tag{3}$$

where $\Delta\mathrm{l}$ is the length of the segments, and $q_j(k)$ is the HTF pump volumetric flow rate on loop j at time instant $(k)\Delta\mathrm{T}$.

2.3. Disturbances and time-varying parameters

The corrected DNI $I_{i,j}(k)$ and the ambient temperature $T^{\mathrm{a}}(k)$ are disturbances that have to be measured or estimated for each time instant.

The coefficient of thermal losses $H^{\mathrm{l}}_{i,j}(k-1)$, the convective heat transfer coefficient of pipe interior $H^{\mathrm{t}}_{i,j}(k-1)$, the density of the fluid $\rho^{\mathrm{f}}_{i,j}(k-1)$, and the specific heat capacity of the fluid $C^{\mathrm{f}}_{i,j}(k-1)$ are computed for each instant based on the current temperature and flow rate of the fluid on the corresponding segment i of loop j.

2.4. Boundary equations

Additionally to the previously shown dynamic equations, a boundary equation is defined for the first segment of each loop:

$$T^{\mathrm{f}}_{1,j}(k) = T^{\mathrm{in}}(k)\ \forall k, j \tag{4}$$

where $T^{\mathrm{in}}(k)$ is the inlet temperature, which is considered (from the point of view of the control system) as a disturbance that has to be measured or estimated for each instant.

Moreover, the outlet temperature ($T^{\mathrm{out}}(k)$) and the total flow rate ($q^{\mathrm{T}}(k)$) can be computed using the following equations:

$$T^{\mathrm{out}}(k) = \sum_{j=1}^{\mathrm{N_l}} \frac{q_j(k) T^{\mathrm{f}}_{j,\mathrm{N}}}{q^{\mathrm{T}}(k)} \tag{5}$$

$$q^{\mathrm{T}}(k) = \sum_{j=1}^{\mathrm{N_l}} q_j(k)\ \forall\ k \tag{6}$$

2.5. Operational constraints

Finally, the following operational constraints have been also considered:

- Constraints on the flow of each line:

  $$q^{\min} \leq q_j(k) \leq q^{\max}\ \ \forall k \text{ and } j \tag{7}$$

  where $q^{\min}$ and $q^{\max}$ are the maximum and minimum values for the flow rate for each loop, which are chosen based on the Reynolds Number and the maximum pressure drop on each loop, respectively.

- Constraints on the total flow:

  $$q^{\mathrm{T}}(k) \leq q^{\mathrm{T,max}}\ \ \forall\ k \tag{8}$$

  where $q^{\mathrm{T,max}}$ is the maximum value allowed for the total flow rate, usually given by the characteristics of the HTF pumps and the hydraulic system connected to them.

- Constraints on the outlet temperature:

  $$T^{\mathrm{f,min}} \leq T^{\mathrm{f}}_{\mathrm{N},j}(k) \leq T^{\mathrm{f,max}}\ \ \forall\ k \text{ and } j \tag{9}$$

  where $T^{\mathrm{f,min}}$ and $T^{\mathrm{f,min}}$ are the minimum and maximum values allowed for the temperature of the HTF.

In this work, it has been assumed that any constraint on the value of the outlet temperature $T^{\text{out}}(k)$ is also constraining the outlet temperature of each loop $T^{\text{f}}_{i,\text{N}}(k)$ using equation (9). This assumption allows to substantially ease the computation of the optimization while ensuring that the outlet temperature constraint is never violated. However, in some particular cases, this assumption could slightly decrease the maximum achievable thermal power. In a future work, this effect will be studied and an specifically designed distributed MPC controller will be proposed in order to optimally deal with these particular cases.

3. Centralized MPC for Concentrated Solar Plants

3.1. Motivation

Commercial plants, and most previously published works, are usually operated at the maximum temperature allowed by the environmental and security conditions. The main reason is that the power cycle increases its efficiency at high temperatures. However, the thermal losses of the solar field ($H^{\text{l}}_{i,j}(k)$) increase with the operating temperature and therefore, working at high temperatures does not necessarily increases the overall efficiency of the combination PCS + solar collector field [11]. This is deeply explained in [8], where it is shows by simulation that the optimum outlet temperature set-point depends on the DNI and the maximum efficiency is not generally achieved at the highest temperature.

Accordingly, the main goal of the controlled proposed in this paper is to maximize the net thermal power provided by the collector field. However, in contrast with [8], in this paper it is assumed that the provided thermal power will be fully employed by the rest of the power plant in order to produce the maximum amount of electrical energy, thanks to the energy storage provided by the TES.

If desired, other terms affecting to the produced electrical energy (such as the oil pump consumption or the efficiency of the Rankine cycle) can be easily considered, by modifing the used cost function, in a similar way that it was done in [8].

3.2. Cost function

As it was previously explained, Model Predictive Control (MPC) [6], which minimizes a cost function using a receding horizon approach, has shown to substantially improve the performance of the controlled thermal power plant in various simulation studies.

The cost function ($J(k)$) used in this work contains one term for the net thermal power ($W(k_{\text{c}})$) for a certain time instant $k_{\text{c}}\Delta\text{T}$, another term that limits (using a soft constraint in order to make the optimization faster) the maximum value of outlet temperature of each loop, and a third term penalizing the flow rate on

each loop:

$$J(k_{\mathrm{c}}) = \tag{10}$$
$$\left(W(k_{\mathrm{c}}) + \psi \sum_{j=1}^{j=N_{\mathrm{l}}} \left(\max(\frac{T^{\mathrm{f}}_{\mathrm{N},j}(k_{\mathrm{c}}) - T^{\mathrm{f,max}}}{T^{\mathrm{f,max}}}, \frac{T^{\mathrm{f,min}} - T^{\mathrm{f}}_{\mathrm{N},j}(k_{\mathrm{c}})}{T^{\mathrm{f,max}}}, 0)^2 \right) + \epsilon \sum_{j=1}^{j=N_{\mathrm{l}}} \left(q_j(k_{\mathrm{c}}) - q_j(k_{\mathrm{c}}-1) \right)^2 \right.$$

where ψ and ϵ are tuning parameters.

The use of soft constraints (second term of equation (10)) and a large enough value of ψ allows to keep the outline temperature within the constraints whenever that is possible. On the other hand, in the cases that the temperature constraints cannot be satisfied, the controller will minimize the violation of these constraints.

The use of penalties on the variations of the control inputs (third term of equation (10)) is a common practice in MPC in order to achieve a more stable behavior and to avoid unnecessary oscillations. However, if desired, this penalization can be removed by using $\epsilon = 0$.

The net thermal power $W(k_{\mathrm{c}})$ (i.e. the heat power transferred to the TES and/or to the PCS) can be computed using the following equation:

$$W(k_{\mathrm{c}}) = W^{\mathrm{out}}(k_{\mathrm{c}}) - W^{\mathrm{in}}(k_{\mathrm{c}}) \approx \sum_{j=1}^{\mathrm{N_l}} W^{\mathrm{out}}_j(k_{\mathrm{c}}) - \sum_{j=1}^{\mathrm{N_l}} W^{\mathrm{in}}_j(k_{\mathrm{c}}) \tag{11}$$

where $W^{\mathrm{in}}(k_{\mathrm{c}})$ and $W^{\mathrm{out}}(k_{\mathrm{c}})$ are the inlet and outlet power for the entire collector field, and $W^{\mathrm{in}}_j(k_{\mathrm{c}})$ and $W^{\mathrm{out}}_j(k_{\mathrm{c}})$ are the inlet and outlet power of each control loop, which can obtained by using the following equations:

$$W^{\mathrm{out}}_j(k_{\mathrm{c}}) = \rho^{\mathrm{f}}_{\mathrm{N},j}(k_{\mathrm{c}}) C^{\mathrm{f}}_{\mathrm{N},j}(k_{\mathrm{c}}) q_j(k_{\mathrm{c}}) T^{\mathrm{f}}_{\mathrm{N},j}(k_{\mathrm{c}}) \tag{12}$$

$$W^{\mathrm{in}}_j(k_{\mathrm{c}}) = \rho^{\mathrm{f}}_{1,j}(k_{\mathrm{c}}) C^{\mathrm{f}}_{1,j}(k_{\mathrm{c}}) q_j(k_{\mathrm{c}}) T^{\mathrm{in}}(k_{\mathrm{c}}) \tag{13}$$

3.3. Optimization

The optimal solution (i.e. the values of the flow that provide the maximum thermal power) between time steps k_{c} and $k_{\mathrm{c}} + \mathrm{N_p}$ for a given DNI profile and ambient temperature can be found by solving the following optimization problem with cost function $J(k)$ (see (10)), which is used to measure the performance of the system with respect to the flow rate sequences:

$$\min_{q_{\mathrm{t}}(k_{\mathrm{c}})} \sum_{k=k_{\mathrm{c}}}^{k_{\mathrm{c}}+\mathrm{N_p}} J(k) \tag{14}$$

subject to: $q^{\mathrm{min}} < q_j(k_{\mathrm{c}}) < q^{\mathrm{max}} \; \forall \; k_{\mathrm{c}}, j$

$$\sum_{j=1}^{\mathrm{N_l}} q_j(k_{\mathrm{c}}) \leq q^{\mathrm{T,max}} \; \forall \; k_{\mathrm{c}}$$

where $q_t(k_c) = [q_1(k_c), q_1(k_c+1), ..., q_1(k_c+N_u-1), q_2(k), q_2(k_c+1), ..., q_{N_l}(k_c+N_u-1)]$ is the vector containing the flow rate values, k_c is the controller time step corresponding to instant $t = k_c \Delta T_c$, N_p is the prediction horizon, and N_u is the control horizon.

In this work, we directly use as control variables the inlet flow to each loop assuming that the hydraulic dynamic is much faster than the thermal one. However, in real applications, these flows will be used as set-points for simple low-level controllers used for each valve and pumps.

The necessary optimizations have been computed using Sequential Quadratic Programming (SQP). It has to be pointed out that, in general, it is necessary to run the optimization algorithms many times (with different initial points) in order to avoid ending up in local minima (because the problem is highly non-convex). More concretely, in this paper, 4 initial points have been used for each computation of the optimal solution (the profile computed in the previous controller time step shifted one time step, the lower bound, the upper bound and one random initial point).

3.4. Model simplifications

Moreover, in order to ease the computation of the optimal solution, a few additional simplifications have been considered:

- The step time and the segments length are modified in order to fasten the time needed for the simulation of the controller.
- The losses are precomputed for a set of temperature and flow values.
- The controller time step is chosen as a multiple of the model time step ($\Delta T_c = \alpha \Delta T$ where α is a positive integer), which is limited due to the discretization.

3.5. Computational complexity

The simplifications explained in the previous subsection allow to substantially decrease the computational time needed for each simulation of the system and, therefore, to reduce the computational time needed for the entire optimization.

However, although the computation of the optimal solution for one loop (with N_u decision variables) can be done relatively fast for short control horizons, the centralized solution (with N_l x N_u decision variables) still needs a long time to be computed making difficult to calculate the optimal value in real time. In fact, the main drawback of MPC is that the computation time quickly increases with the size of the network, making it difficult to apply centralized MPC for large power plants. In order to overcome this practical problem, a distributed architecture for the MPC controller is proposed in the following Section.

4. Distributed MPC for Concentrated Solar Plants

4.1. Motivation

As previously explained, a properly designed distributed MPC can approach the performance of a centralized MPC while reducing the computational load allowing to implement an MPC controller in real time for large networked systems.

Distributed MPC architectures have been already successfully proposed and used for many kinds of networked systems, such as traffic systems [12], electrical networks [13], irrigation canals [14] and many others applications.

In the case of parabolic-though collector field, it is possible to take advantage of some characteristics of the mathematical model of the network in order to propose a fast distributed MPC that can approach the global solution.

Concretely, as it can be seen in equation (11), the maximization of the net thermal power of the plant is nearly equal to the maximization of the summation of the thermal powers provided by each loop.

Therefore, in the absence of global constraints, there is not direct coupling on the maximization of the thermal powers of each line (i.e. a decentralized controller with reach the optimal solution). However, there is one global constraint that creates a significant coupling between the loops of the collector field: The maximum of value of the total flow $q^{\mathrm{T,max}}$ is bounded as it can be seen in equation (8).

This constraint will cause a large discrepancy between a centralized and a fully decentralized (local) MPC in the cases that the plant is unbalanced (i.e. the flow rates of some loops are higher than the flows of other loops).

This unbalanced operation of the collector field can be desired (improving the performance) in the cases when there is a high discrepancy between the DNI and/or the efficiency of the loops. In these cases, the thermal power can be increased by reducing the flow in some loops (the ones with the lowest DNI or efficiency) and increasing the flow in others (the most sunny ones or efficient ones) while keeping the total flow in its maximum value.

4.2. Control structure

As explained in the previous subsection, it can be said that the only coupling (from the point of view of the optimization) between the loops of the collector field, is the coupling on the inputs (the summation of the flow rates in each loop has to be lower than the maximum allowed total flow rate).

Taking advantage of this limited coupling, a logic-based distributed MPC controller (see Figure 2) has been proposed in order to approach the performance of a centralized MPC:

- Firstly, the controller solves the local optimization problem for each loop.

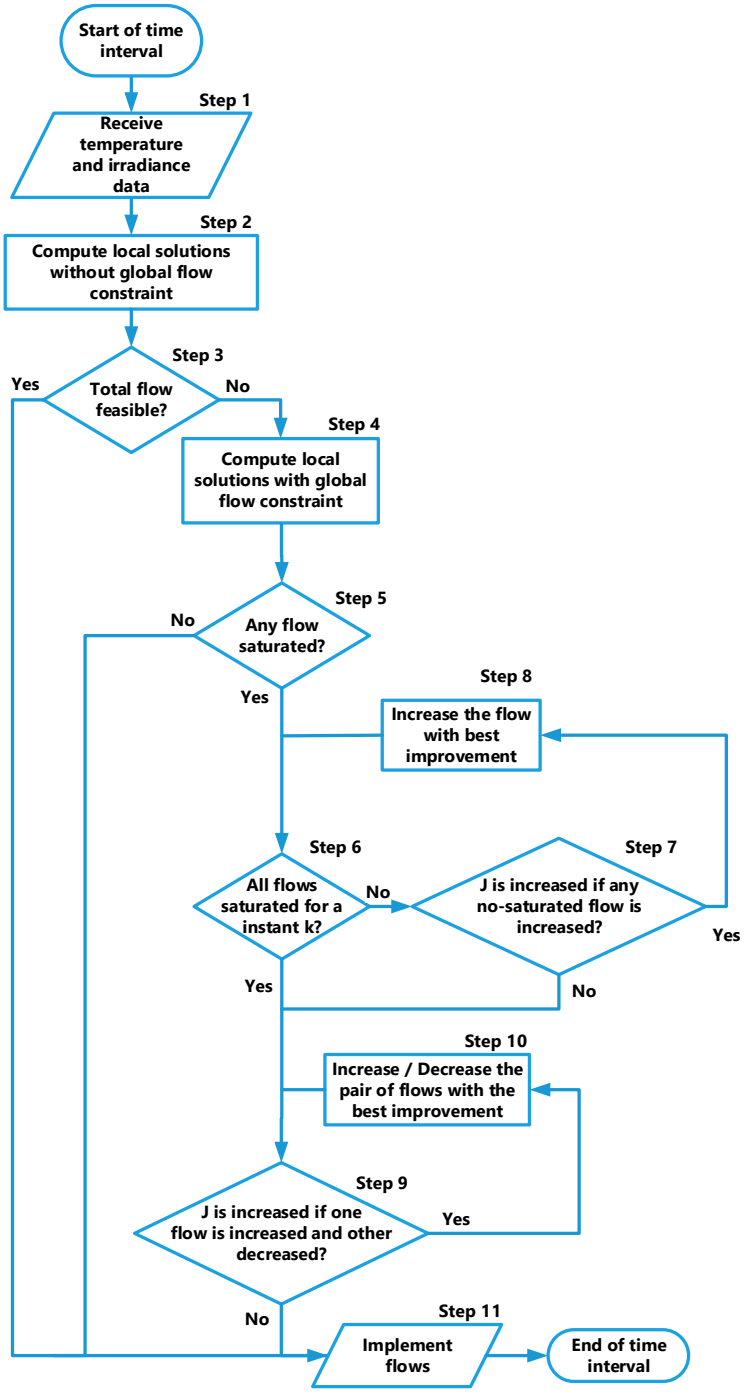

Figure 2: Distributed logic-based algorithm for solar parabolic-trough plants

- Then, if the obtained solution is not globally feasible, the local optimizations are recomputed but limiting their flows in order to ensure that the obtained flows are feasible for the entire collector field.
- However, the obtained feasible solution is not necessarily optimal. Therefore, an iterative procedure is then carried on to increase the optimality of the obtained flows while ensuring feasibility.

4.3. Control algorithm

The proposed algorithm is composed by the following steps:

- **Step 1:** The temperatures and DNI measurements are received and the future DNI and ambient temperature profiles are estimated.
- **Step 2:** This step finds, one by one, the flow rate for each loop j given by a local MPC without any global constraint. This flow rate is found by solving the MPC problem explained in Section 3 but using a local cost function and only one flow rate as a decision variable:

$$\min_{q_{\mathrm{l},j}(k_\mathrm{c})} \sum_{k=k_\mathrm{c}}^{k_\mathrm{c}+\mathrm{N_p}} J_j^\mathrm{L}(k) \tag{15}$$

subject to: $q^{\min} < q_j(k_\mathrm{c}) < q^{\max}\ \forall k_\mathrm{c}, j$

where $q_{\mathrm{l},j}(k_\mathrm{c}) = [q_j(k_\mathrm{c}), q_j(k_\mathrm{c}+1), ..., q_j(k_\mathrm{c}+N_{\mathrm{s}-1})$ is the vector containing the flow rate values for loop j along the control horizon and $J_\mathrm{l}(k_\mathrm{c})$ is the local cost function:

$$J_j^\mathrm{L}(k) = \tag{16}$$
$$\sum_{k_\mathrm{c}}^{k_\mathrm{c}+\mathrm{N_p}} \left(W_j(k_\mathrm{c}) + \max\left(\frac{T^\mathrm{f}_{\mathrm{N},j}(k_\mathrm{c}) - T^{\mathrm{f,max}}}{T^{\mathrm{f,max}}}, \frac{T^{\mathrm{f,min}} - T^\mathrm{f}_{\mathrm{N},j}(k_\mathrm{c})}{T^{\mathrm{f,max}}}, 0\right)^2 + \epsilon\Big(q_j(k_\mathrm{c}) - q_j(k_\mathrm{c}-1)\Big)^2 \right)$$

- **Step 3:** This step checks if the solution obtained in Step 2 is feasible (and, therefore, optimal) or not:

  if $q^\mathrm{T}(k_\mathrm{c}) \leq q^{\mathrm{T,max}}\ \ \forall\ k_\mathrm{c}$ **then**

  Go to Step 11

  else

  Go to Step 4

  end if

- **Step 4:** The local MPC solution for each loop j is computed again (like in Step 2) but, in this step, the maximum allowed flow rate is changed to $\frac{q^{\mathrm{T,max}}}{N_l}$ resulting in the following optimization problem:

$$\min_{q_{\mathrm{l},j}(k_\mathrm{c})} \sum_{k=k_\mathrm{c}}^{k_\mathrm{c}+\mathrm{N_p}} J_j^\mathrm{L}(k) \tag{17}$$

subject to: $q^{\min} < q_j(k_\mathrm{c}) < \dfrac{q^{\mathrm{T,max}}}{N_l}\ \forall k_\mathrm{c}$

This step allows to obtain a feasible, but not necessarily optimal, solution for the centralized problem.

- **Step 5:** This step checks if the solution obtained in Step 4 is optimal or not (the solution obtained for each loop with be optimal if, and only if, the obtained flow rate is not saturated for any instant along the control horizon):

  if $q_j(k_c) \leq q^{\max} \ \ \forall\ k_c$ and j **then**

  Go to Step 11

  else

  Go to Step 6

  end if

- **Step 6:** This steps checks if the total flow is equal to the maximum flow (in which case, in order to increase the flow rate for one loop is necessary to decrease the flow rate for another loop) or if the total flow is lower than than the maximum (in which case, the flow rate of saturated loop can be increased using the margin between the current total flow rate and the maximum one).

  if $q^{\mathrm{T}}(k_c) = q^{\mathrm{T,max}} \ \ \forall\ k_c$ **then**

  Go to Step 9

  else

  Go to Step 7

  end if

- **Step 7:** This step checks if the cost function can be increased by increasing the flow rate of one loop during the first control instant.

  Compute the increment in the local cost functions obtained by increasing the corresponding flow rate of loop j:

$$\Delta J_j^L(k_c) = J(q_{l,j}(k_c) + \Delta q_{l,j}(k_c)) \tag{18}$$

$$\text{where } \Delta q_{l,j}(k_c) = \begin{cases} \lambda & \text{if } k_c = 1 \\ 0 & \text{Otherwise} \end{cases}$$

  if $\max\left(\Delta J_j^L(k_c)\right) > 0$ **then**

  Go to Step 8

  else

  Go to Step 9

  end if

  It is not necessary to check the loops that are not saturated since the current solution (given by Step 4) is already optimal (from a local point of view).

- **Step 8:** This step increases the flow rate of a loop within the available total flow. More concretely, the flow of the loop with highest improvement on the cost function is sequentially increased until the obtained improvement on the cost function is lower than the one obtained increasing another loop, until the total flow is equal to the maximum one or until the cost function is not significantly improved.

  Select the loop j_{inc} with the highest value of $\Delta J_j^L(k_{\text{c}})$. Define $\Delta \bar{J}^L(k_{\text{c}})$ as the second highest value of $\Delta J_j^L(k_{\text{c}})$.

  while $\Delta J_{j_{\text{inc}}}^L(q_{j_{\text{inc}}}(k_{\text{c}})) > \Delta \bar{J}^L(k_{\text{c}})$ & $q^{\text{T,max}} > \sum_{j=1}^{j=N_l} q_{l,j}(k_{\text{c}})$ **do**

  $q_{j_{\text{inc}}}(k_{\text{c}}) = q_{j_{\text{inc}}}(k_{\text{c}}) + \min\left(\lambda, q^{\text{T,max}} - \sum_{j=1}^{j=j_{\text{inc}}-1} q_{l,j}(k_{\text{c}}) - \sum_{j=j_{\text{inc}}+1}^{j=N_l} q_{l,j}(k_{\text{c}})\right)$

  end while

- **Step 9:** This steps checks if the cost function can be increased by increasing the flow rate of one loop and decreasing, in the same quantity, the flow rate in another one.

  Compute $J_j^L(k_{\text{c}})$.

  Compute the increment in the local cost functions obtained by increasing the corresponding flow rate of loop j using eq. (18).

  Compute the decrement in the local cost functions obtained by decreasing the corresponding flow rate of loop j:

$$\bigtriangledown J_j^L(k_{\text{c}}) = J(q_{l,j}(k_{\text{c}}) + \bigtriangledown q_{l,j}(k_{\text{c}})) \tag{19}$$

$$\text{where } \bigtriangledown q_{l,j}(k_{\text{c}}) = \begin{cases} -\lambda & \text{if } k_{\text{c}} = 1 \\ 0 & \text{Otherwise} \end{cases}$$

  if $\max\left(\Delta J_j^L(k_{\text{c}})\right) > \min\left(\bigtriangledown J_j^L(k_{\text{c}})\right)$ **then**

  Go to Step 10

  else

  Go to Step 11

  end if

- **Step 10:** This step increases the flow rate of a loop decreasing in the same amount the flow rate of another loop. More concretely, the flow of the loop with the highest improvement on the cost function is sequentially increased (and the flow of the loop with with the lowest worsening is decreased) until the obtained improvement on the cost function is lower than increasing/decreasing another loops or until the cost function is not significantly improved.

  Select the loop j_{inc} with the highest value of $\Delta J_j^L(k_{\text{c}})$ and the loop j_{dec} with the lowest value of $\bigtriangledown J_j^L(k_{\text{c}})$. Define $\Delta \bar{J}^L(k_{\text{c}})$ and $\bigtriangledown \bar{J}^L(k_{\text{c}})$ as the second highest value of $\Delta J_j^L(k_{\text{c}})$ and $\bigtriangledown J_j^L(k_{\text{c}})$.

  while $\left(\Delta J_{j_{\text{inc}}}^L(q_{j_{\text{inc}}}(k_{\text{c}})) - \bigtriangledown J_{j_{\text{inc}}}^L(q_{j_{\text{inc}}}(k_{\text{c}}))\right) > \left(\Delta \bar{J}^L(k_{\text{c}}) - \bigtriangledown \bar{J}^L(k_{\text{c}})\right)$ **do**

$$q_{j_{\mathrm{inc}}}(k_{\mathrm{c}}) = q_{j_{\mathrm{inc}}}(k_{\mathrm{c}}) + \lambda$$
$$q_{j_{\mathrm{dec}}}(k_{\mathrm{c}}) = q_{j_{\mathrm{dec}}}(k_{\mathrm{c}}) - \lambda$$

end while

- **Step 11:** The obtained values for the flow rates are implemented.

5. Results

5.1. Case-study

The MPC controllers proposed in this paper have been simulated for the collector field ACUREX, which was located at the Plataforma Solar de Almería (PSA) in Spain. This parabolic-though CST plant has been used as a case-study in many previous research works such as [15, 16, 4, 2].

The model of the collector field used for the simulations done in this paper is composed of 10 loops ($\mathrm{N_l} = 10$) with a length of 174 meters. Each loop is discretized into 174 segments ($\mathrm{N} = 170$) with a length of 1 meter ($\Delta \mathrm{l}_{i,j} = 1\ \mathrm{m}\ \forall\ i,j$). Segments $\{37, 42\}$, $\{79, 96\}$, and $\{133, 138\}$ are passive parts (joints and other parts not reached by concentrated radiation) and therefore their DNI are set to 0 as it can be seen in Fig. 3.

In this paper (like in most previous references), Therminol Vp1 is used for the HTF. The fluid density $\rho^{\mathrm{f}}_{i,j}(k)$ and specific heat capacity $C^{\mathrm{f}}_{i,j}(k)$ are determined for each instant based on the temperature of the HTF on the corresponding segment:

$$\rho^{\mathrm{f}}_{i,j}(k) = 903 - 0.672 T^{\mathrm{f}}_{i,j}(k) \tag{20}$$
$$C^{\mathrm{f}}_{i,j}(k) = 1820 + 3.478 T^{\mathrm{f}}_{i,j}(k) \tag{21}$$

The coefficient of thermal losses $H^{\mathrm{l}}_{i,j}(k-1)$ and the convective heat transfer coefficient of pipe interior $H^{\mathrm{t}}_{i,j}(k-1)$ are also computed for each time instant based on the temperature of the HTF on the corresponding segment, the flow on the corresponding loop and the ambient temperature [2]:

$$H^{\mathrm{l}}_{i,j}(k) = 0.00249(T^{\mathrm{f}}_{i,j}(k) - T^{\mathrm{a}}(k)) - 0.06133 \tag{22}$$

$$H^{\mathrm{t}}_{i,j}(k) = \tag{23}$$
$$q_j(k)^{0.8}\left(2.17 \cdot 10^6 - 5.01 \cdot 10^4 T^{\mathrm{f}}_{i,j}(k) + 4.53 \cdot 10^2 {T^{\mathrm{f}}}_{i,j}(k)^2 - 1.64 {T^{\mathrm{f}}}_{i,j}(k)^3 + 2.1 \cdot 10^{-3} {T^{\mathrm{f}}}_{i,j}(k)^4\right)$$

As explained in Section 3, the computation of the convective heat transfer coefficient, within the MPC computation, has been be precalcuted for an array of values of fluid temperature and flow in order to decrease the computational load needed for the calculation of the optimal solution. On the other hand, for the simulation of the collector field, the convective heat transfer coefficient has be exactly computed for each segment and instant using (23).

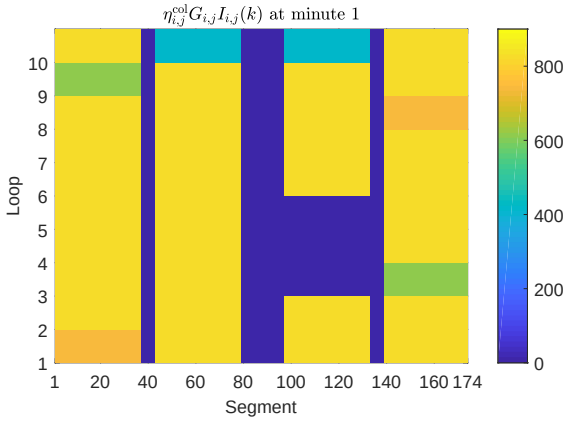

Figure 3: Effective DNI on the collector field with no clouds

The values of the rest of the model parameters (the ones that have the same value for each segment and time instant) are shown in Table 1.

Table 1: ACUREX Model Parameters

ΔT	0.5 s	ρ^{m}	7800 kg/m^3
C^{m}	550 J/(Kg°C)	D^{m}	0.031 m
D^{f}	0.0254 m	A^{m}	2.4810^{-4} m^2
A^{f}	7.5510^{-4} m^2		

In order to find the value of optimal control inputs that maximizes a cost within a prediction horizon, it is necessary to provide the MPC controller with the current and future values of the disturbances. In the case of collectors solar field, these disturbances are the ambient temperature and the effective DNI, which is obtained by multiplying the efficiency of the collectors, the aperture of the collectors and the corrected DNI (see equation (1)).

In this paper, the ambient temperature is considered to be equal to 25°C for any segment and instant. On the other hand, a two-hour effective DNI profile that changes with space and time ($\eta_{i,j}^{\mathrm{col}} G_{i,j} I_{i,j}(k)$) is used for simulation of the collector field:

- During most of the simulation (from minute 1 to minute 62 and from minute 77 to minute 120), the effective DNI does not change with time. However, for some segments (such as the first 36 segments of loops 1 and 9), a decreased efficiency is used (in order to model dirty or defocused collectors), entailing lower effective DNI as it can be seen in Fig. 3.

- From minute 63 to minute 76, a moving cloud appears (firstly affecting segment 10) entailing a significant reduction in the effective DNI. By way of example, Fig. 4 shows the effective DNI affecting

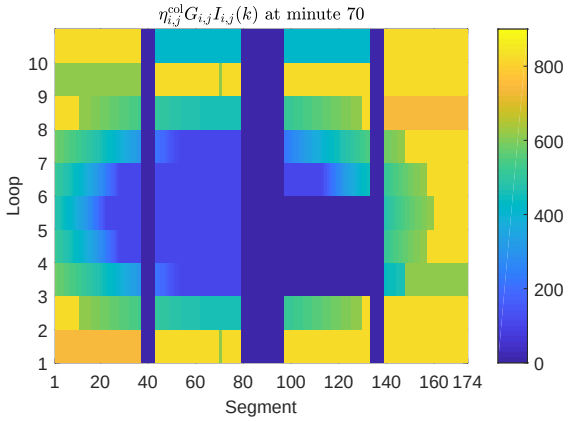

Figure 4: Effective DNI on the collector field with affected by the cloud considered at minute 70

the collector field at minute 70. Based in our experience, the used moving cloud is a representative example of small cumulus moving in light air, which recurrently affect solar collector fields during partially clouded days. In future works, other kinds of clouds will be considered (such as stratus or cumulonimbus that fully cover the collector field).

The inlet temperature is computed based on the outlet temperature according to the following equation:

$$T^{\text{in}}(k) = 0.999167 T^{\text{in}}(k-1) + 0.000833(T^{\text{out}}(k-1) - 90) \tag{24}$$

This equation results from the discretization of a linear first-order system with a time constant of 10 minutes and discretization step of 0.5 seconds:

$$\frac{T^{\text{in}}(s)}{\hat{T}^{\text{out}}(s)} = \frac{1}{600s+1} \tag{25}$$

with $\hat{T}^{\text{out}}(t) = T^{\text{out}}(t) - 90$

For the computation of the local MPC solutions (needed in Steps 2 and 4 of the Distributed algorithm), equation (25) has to be modified since the future values of the outlet temperature are unknown. In order to deal with this problem, the last measured value for the outlet temperature $T^{\text{out}}(k_{\text{c}})$ is used for the entire prediction horizon $\{k_{\text{c}}, k_{\text{c}}+1, ..., k_{\text{c}}+\text{N}_{\text{p}}\}$.

For this case study, ψ and ϵ have been set equal to 450 and 30, respectively, for the centralized MPC. For the Local MPC (and, therefore, for the Distributed MPC), ψ and ϵ have been set equal to 45 and 3, respectively. If lower values of ϵ and/or Ω are used, the TTS is slightly reduced, but in general higher oscillations may appear in the control signals.

The control step time used for the MPC controllers is equal to one minute, entailing a value of α equal to 20. The prediction and control horizons are set equal to 12 minutes ($\text{N}_{\text{p}} = 12$) and 10 minutes ($\text{N}_{\text{u}} = 10$),

respectively. The step time of the model used for control is equal to 3 s and the used segment lenght is equal to 6 m.

Finally, the values used for the operational constraints considered in this paper are shown in Table 2:

Table 2: Operational constraints

$q^{\max}$	0.2 l/s	$q^{\min}$	1.5 l/s	$q^{\mathrm{T,max}}$	12 l/s
$T^{\mathrm{f,max}}$	220°C	$T^{\mathrm{f,min}}$	300°C		

5.2. Numerical results

Apart from the previously explained controllers (Centralized MPC and Distributed MPC), four other control architectures have been tested:

- **Local MPC:** This controller find the local MPC limiting the flow in order to make the global solution (like in the Step 3 of the distributed algorithm).
- **Local MPC maximizing T:** For this MPC controller, the cost function is switched to a new one that maximizes the outlet temperature (subject to the same constraints that the other controllers) instead of maximizing the net thermal power.
- **Local MPC minimizing T:** Equivantely, in this case the cost function is switched to a new one that minimizes the outlet temperature instead of maximizing the net thermal power.
- **No-valves:** This MPC controller computes the centralized solution but assuming that the same flow rate is applied to the entire set of loops (i.e. the valves cannot be controlled).

The numerical results for the considered case study are shown in Table 3. The no valves case is used as a baseline for the comparison since it corresponds to the most frequently used control architecture for the collector fields of parabolic-trough CST plants.

In the results in Table 3 it can be seen that, as expected, the centralized controller provides the best performances, therefore entailing an mean thermal power improvement, during the two hours of simulation, of the 1.09 % comparing with the no-valves case. On the other hand, the computational load is too high to implemented in real time. More concretely, the mean computation time that is needed to compute the control inputs for each controller step is 240.3 s.

The computation times may be reduced improving the code (for example, using C instead of MATLAB) and/or using a faster processor. As a result, it would be possible to compute the centralized solution in real-time for a small collector field like ACUREX. However, since the computation time increase exponentially, a MPC centralized controller is impracticable for large collector fields.

Table 3: Mean thermal power obtained for different controllers

Controller	Mean power	Improvement
No-valves	1118.6 kW	0 %
Local MPC	1126.6 kW	0.72 %
Local MPC minimizing T	1123.6 kW	0.45 %
Local MPC maximizing T	1070.9 kW	-4.26 %
Distributed MPC	1130.4 kW	1.05 %
Centralized MPC	1130.8 kW	1.09 %

On the other hand, the computational load using the proposed distributed MPC controller is much lower (with a mean computation time of 17.3 s) allowing an implementation in real-time. However, at the same time, the distributed MPC is able to approach the performance achieved by the centralized controller (with a mean power improvement of a 1.05 %, only a 0.04 % worse than using the centralized MPC). It is worth to mention that Steps 1 and 3 (the ones that takes most of the computational load) may be computed in parallel, substantially reducing the global computation time. More concretely, if Steps 1 and 3 are computed in parallel the mean computation time is 5.2 s.

The Local MPC controller provides an acceptable solution but with a significant reduction in the thermal power achieved (with an 0.37 % mean power reductions comparing with the centralized MPC). Nevertheless, the solution is still much better that the one achieved without using valves on each loop (as it is usually done in current commercial plants). In fact, without individually controlling the valves, the performance is reduced in a 0.72 %.

Finally, in Table 3 it can be seen that the maximization of the outlet temperature (which have been used in many works and commercial plants) implies a high loss of performance (4.26 % with respect to the no-valves case). On the other hand, to minimize the outlet temperature implies an acceptable performance (only a 0.27 % worse than the Local MPC).

The evolution of flows and outlet temperatures for the case study considered are shown in Fig. 5, Fig. 6, Fig. 7, and Fig. 8.

Firstly, the flows obtained using a Local MPC controller and the corresponding temperatures are shown in Fig. 5. It can be seen that the controller tries to reduce the temperatures of the entire set of loops. However, due to the maximum flow that can be applied in each loop (0.65 l/s), only the temperatures of 3 loops (the ones with the lowest effective DNI) reach the minimum temperature constraint of 220°C.

In contrast, for the Distributed MPC controller the temperatures of all loops reach the minimum temperature constraint as it can be seen in Fig. 6. This is achieved by increasing the flow of the saturated loops using the margin provided by the other 4 segments (Loops 3,4,5 and 10).

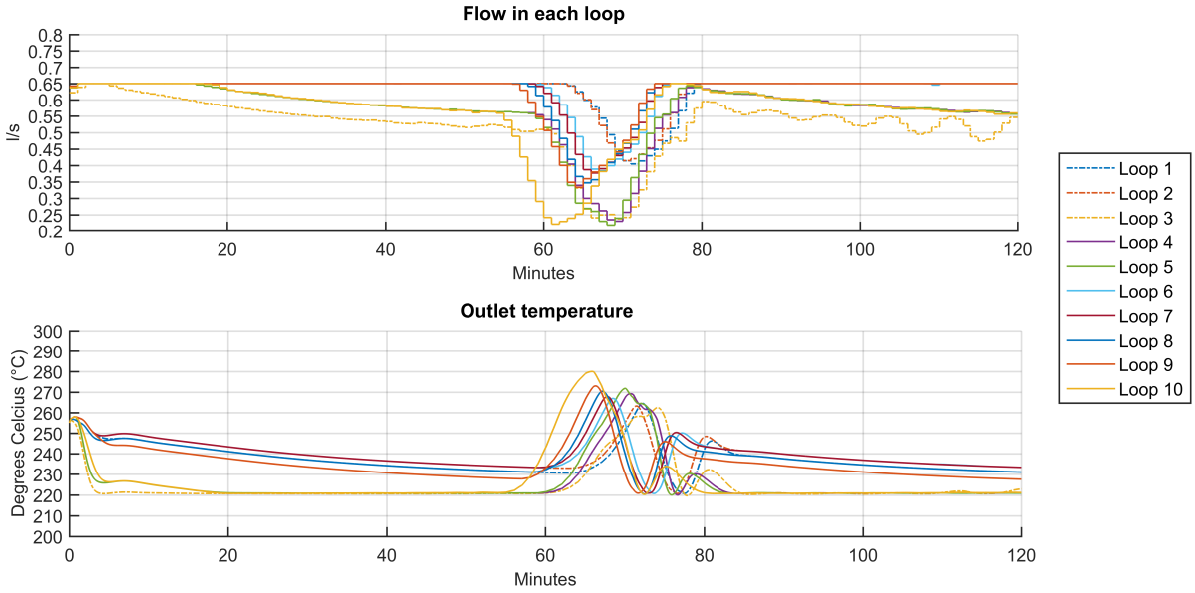

Figure 5: Flow and outlet temperature for each line of the plant (each line is represented by one color) using Local MPC.

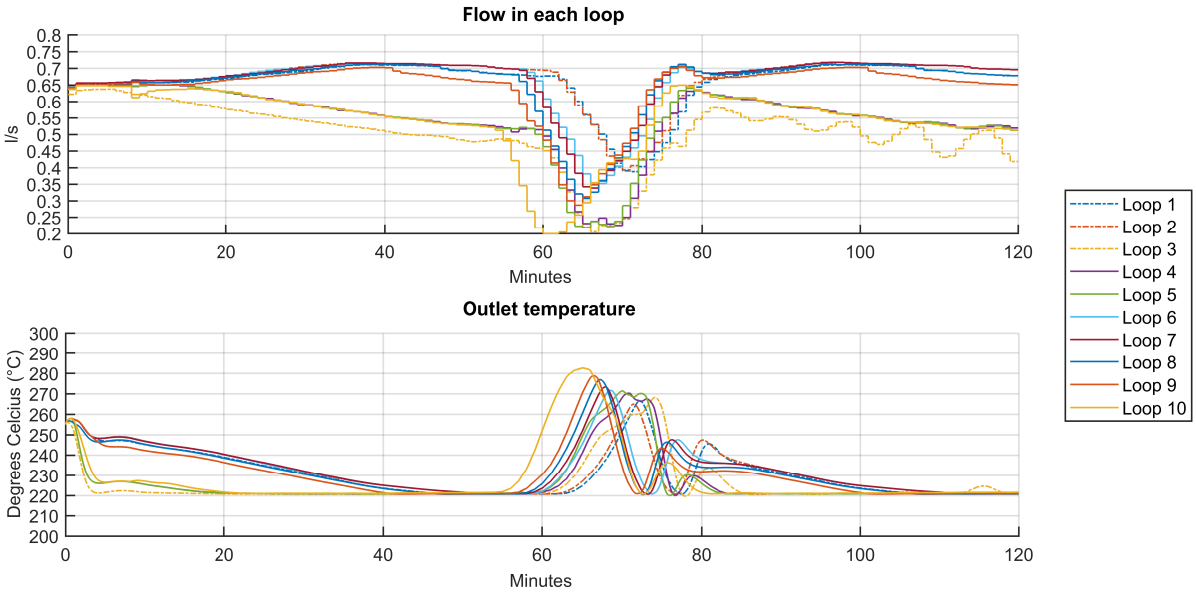

Figure 6: Flow and outlet temperature for each line of the plant (each line is represented by one color) using Distributed MPC.

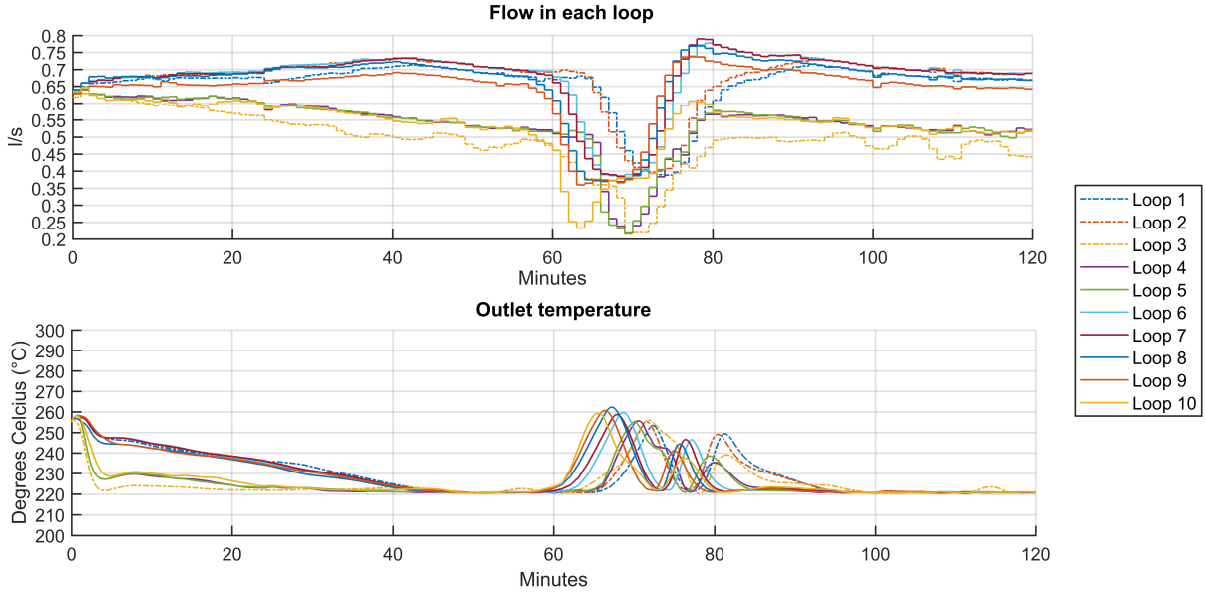

Figure 7: Flow and outlet temperature for each line of the plant (each line is represented by one color) using Centralized MPC.

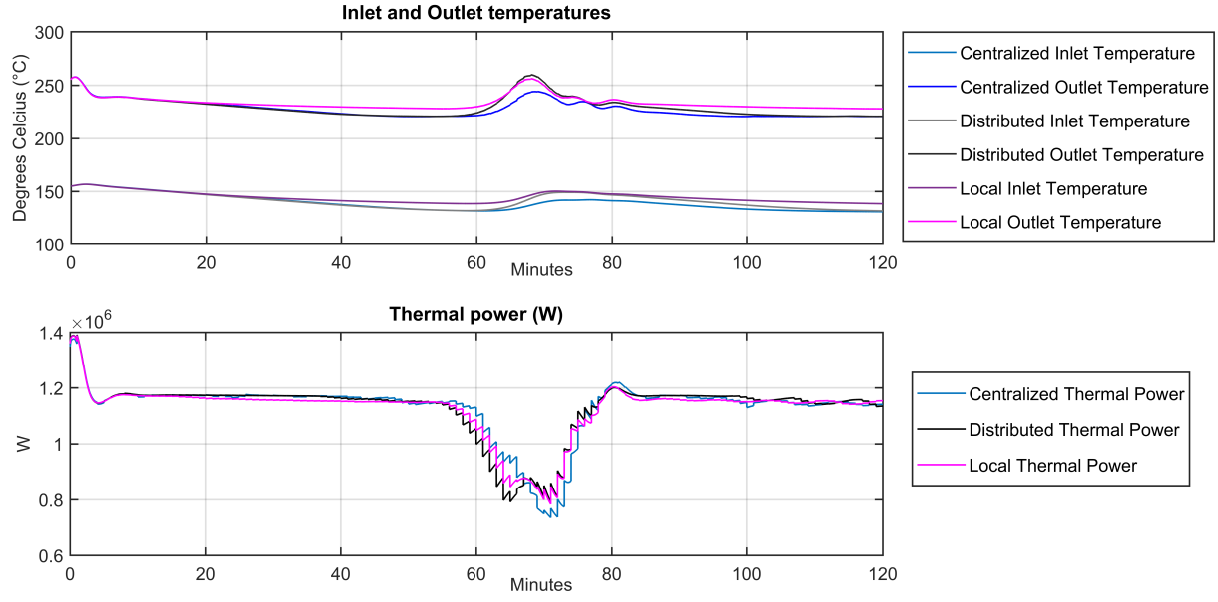

Figure 8: Flow and outlet temperature for each line of the plant (each line is represented by one color) using Distributed MPC.

Subsequently, Fig. 7 shows the flows obtained using a Centralized MPC controller and the corresponding temperatures. The result obtained is very similar to the one obtained with the Distributed MPC during most of the simulation. However, the centralized MPC controller is able to better deal with the cloud appearing between minutes 60 and 80. In fact, the maximum temperature achieved during this transitory is around 260°C, while for the distributed MPC is around 280°C.

This increase in the temperatures is induced by the predictive controller in order to anticipate the future decrease in the temperatures due to the approaching cloud. This prediction relays on the estimation of the future values of the DNI on the collector field.

Finally, Fig. 7 shows the total inlet and outlet temperatures for the collector field and thermal power achieved for each instant using Local, Distributed and Centralized MPC. It can be seen that the thermal power achieved by the Distributed MPC is almost the same that the one achieved with the centralized controller when there is no cloud but they differ substantially when the cloud appear between minutes 60 and 80.

6. Conclusion

This paper has proposed two new MPC algorithms for the maximization of the thermal power of parabolic-trough collector fields equipped with valves located at the beginning of each loop of collectors:

- Firstly, a centralized MPC is proposed. The main particularities of the proposed controller are the direct maximization of the obtained thermal power (i.e. without using a set-point for the outlet temperature) and the use of control valves at the beginning of each loop.

- Subsequently, a logic-based distributed MPC controller has been proposed. This controller approaches which approaches the performance of the centralized MPC but with a much faster computational of the control inputs.

The controllers have been tested using a model of the collector field ACUREX, which was located in Almería, Spain. A synthetic DNI profile, which include a small cloud covering parts of the collector field during a few minutes, was used for the simulation of the thermal system and for the predictions of the MPC controllers.

The obtained results show that the achieved thermal power is significantly lower using a local MPC than using a centralized MPC, entailing a loss of 4.2 kW (0.37%). On the other hand, the proposed distributed MPC is able to perform close to the centralized one, with a small loss of 0.1 kW.

The numerical results also show that the obtained thermal power is decreased in 7.2 kW (0.64%) if the flow is maximized and in 59.5 kW (5.3%) if the outlet temperature is maximized. This shows that, although

both choices are suboptimal, to operate the system at low outlet temperatures is much more acceptable (in terms of thermal power) than to operate the system at high temperatures.

In future works, the computation of the Local MPC solution (needed for the distributed MPC) will be significantly fasten by using neural networks or other optimization algorithms (such as gradient-based ones). Moreover, other distributed architectures (such as coalitional control) will be proposed and tested, the economic benefits of the use of valves will be analyzed and the use a detailed hydraulic model of the system will be studied.

References

[1] C. B. Field et. al., Climate change 2014: impacts, adaptation, and vulnerability, IPCC WGII AR5: Summary for policy-makers.

[2] E. F. Camacho, M. Berenguel, F. R. Rubio, D. Martinez, Control of solar energy systems, Advances in Industrial Control Springer.

[3] REN 21, Renewables: Global status report 2018, http://www.ren21.net/wp-content/uploads/2018/06/17-8652_GSR2018_FullReport_web_-1.pdf.

[4] E. F. Camacho, F. R. Rubio, M. Berenguel, L. Valenzuela, A survey on control schemes for distributed solar collector fields. Part I: modeling and basic control approaches, Solar Energy 81 (2007) 1240–1251.

[5] E. F. Camacho, F. R. Rubio, M. Berenguel, L. Valenzuela, A survey on control schemes for distributed solar collector fields. Part II: advanced control approaches, Solar Energy 81 (2007) 1252–1272.

[6] E. F. Camacho, C. Bordons, Model predictive control, Springer Verlag.

[7] E. F. Camacho, A. J. Gallego, Model predictive control in solar trough plants: A review, 5th IFAC Conference on Nonlinear Model Predictive Control, Seville, Spain. IFAC-PapersOnLine 48 (23) (2015) 278–285.

[8] E. F. Camacho, A. J. Gallego, Optimal operation in solar trough plants: A case study, Solar Energy 95 (2013) 106–117.

[9] A. J. Sánchez, A. J. Gallego, J. M. Escaño, E. F. Camacho, Temperature homogenization of a solar trough field for performance improvement, Solar Energy 165 (2018) 1–9.

[10] S. J. Navas, F. R. Rubio, P. Ollero, J. M. Lemos, Optimal control applied to distributed solar collector fields with partial radiation, Solar Energy 159 (2018) 811–819.

[11] W. B. Stine, M. Geyer, Power from the sun, http://www.powerfromthesun.net.

[12] J. R. D. Frejo, E. F. Camacho, Global versus local MPC algorithms in freeway traffic control with ramp metering and variable speed limits, IEEE Transactions on Intelligent Transportation Systems 13 (4) (2012) 1556–1565.

[13] R. Halvgaard, L. Vandenberghe, N. K. Poulsen, H. Madsen, J. B. Jorgensen, Distributed model predictive control for smart energy systems, IEEE Transactions on Smart Grid 7 (3) (2016) 1675–1682.

[14] R. R. Negenborn, P. J. van Overloop, T. Keviczky, B. De Schutter, Distributed model predictive control of irrigation canals, Networks and Heterogeneous Media 4 (2) (2009) 359–380.

[15] E. F. Camacho, F. R. Rubio, F. M. Hughes, Self-tuning control of a solar power plant with a distributed collector field, IEEE Control Systems 12 (2) (1992) 72–78.

[16] R. N. Silva, L. M. Rato, J. M. Lemos, F. Coito, Cascade control of a distributed collector solar field, Journal of Process Control 7 (2) (1997) 111–117.